

# Constraints on the Galactic Dark Matter signal from the Fermi-LAT measurement of the diffuse gamma-ray emission

G. Zaharijas

*International Center for Theoretical Physics, Trieste, Italy and  
Institut de Physique Théorique, CEA/Saclay, F-91191 Gif sur Yvette, France*

J. Conrad, A. Cuoco, Z. Yang

*Department of Physics, Stockholm University, AlbaNova, SE-106 91 Stockholm, Sweden and  
The Oskar Klein Centre for Cosmoparticle Physics, AlbaNova, SE-106 91 Stockholm, Sweden*

We study diffuse gamma-ray emission at intermediate Galactic latitudes measured by the Fermi Large Area Telescope with the aim of searching for a signal from dark matter annihilation or decay. In the absence of a robust dark matter signal, constraints are presented. We set both, conservative dark matter limits requiring that the dark matter signal does not exceed the observed diffuse gamma-ray emission and limits derived based on modeling the foreground astrophysical diffuse emission. Uncertainties in several parameters which characterize conventional astrophysical emission are taken into account using a profile likelihood formalism. The resulting limits impact the range of particle masses over which dark matter thermal production in the early Universe is possible, and challenge the interpretation of the PAMELA/Fermi-LAT cosmic ray anomalies as annihilation of dark matter.

## 1. Introduction

Most of the mass in our Universe is in the form of yet un-identified particles (i.e. Dark Matter (DM)) which have been detected only through their gravitational interactions thus far. In one of the most attractive frameworks to explain the DM problem (the WIMP paradigm) those particles are expected to self annihilate to stable standard model particles, producing gamma rays, electrons and protons. Due to our proximity to the center of the Milky Way DM halo, such gamma ray emission originating in our Galaxy would appear as a diffuse signal.

At the same time, the majority of the Galactic diffuse emission is produced through radiative losses of cosmic-ray (CR) electrons and nucleons in the interstellar medium. Modeling of this emission presents one of the major challenges when looking for subdominant signals from dark matter.

In this analysis we test the diffuse LAT data for a contribution from the DM signal by performing a fit of the spectral and spatial distributions of the expected photons at intermediate Galactic latitudes. In doing so, we take into account the most up-to-date modeling of the established astrophysical signal, Ackermann *et al.* [2012,b]. Our aim is to constrain the DM properties and treat the parameters of the astrophysical diffuse gamma-ray background as nuisance parameters. Those parameters are typically correlated with the assumed DM content and it is thus important to scan over them together with the DM parameter space, since they affect directly the DM fit.

Besides this approach, we will also quote conservative upper limits using the data only (i.e. without performing any modeling of the astrophysical background).

## 2. Modeling of the high-energy Galactic diffuse emission

We follow Ackermann *et al.* [2012b] in using the GALPROP code v54 Strong *et al.* [2000], to calculate the propagation and distribution of CRs in the Galaxy and the whole sky diffuse emission, as well as the signal from DM. Several parameters enter the CR propagation modeling, see Ackermann *et al.* [2012b] for more detail: the distribution of CR sources, the half-height of the diffusive halo  $z_h$ , the radial extent of the halo  $R_h$ , the nucleon and electron injection spectrum, the normalization of the diffusion coefficient  $D_0$ , the rigidity dependence of the diffusion coefficient  $\delta$ , ( $D(\rho) = D_0(\rho/\rho_0)^{-\delta}$  with  $\rho_0$  being the reference rigidity) and the Alfvén speed  $v_A$ , (parametrizing the strength of re-acceleration of CRs in the ISM via Alfvén waves) and the velocity of the Galactic winds perpendicular to the Galactic Plane  $V_c$ . Interactions of the CRs with the interstellar medium (ISM) and interstellar radiation field (ISRF) produce three distinct components of the gamma-ray emission: photons from the *decay of neutral pions* produced in the interaction of the CR nucleons with the interstellar gas, *bremsstrahlung* of the CR electron population on the interstellar gas and their *inverse Compton* scattering off the interstellar radiation field.

In Ackermann *et al.* [2012b] various standard parameters of the CR propagation were studied in a fit to CR data and it was shown that they represent well the gamma-ray sky, although various residuals (at a  $\sim 30\%$  level Ackermann *et al.* [2012b]), both at small and large scales, remain. These residuals can be ascribed to various limitations of the models: imperfections in the modeling of gas and ISRF components, simplified assumptions in the propagation set-up, unresolved point sources, and large scale structures like

Loop I Casandjian *et al.* [2009] or the Galactic Bubbles Su *et al.* [2010]. Since residuals do not seem obviously related to DM, we focus in the following on setting limits on the possible DM signal, rather than *searching* for a DM signal.

In our work, we use the results of the fits to the CR data from Ackermann *et al.* [2012b] but we allow for more freedom in certain parameters governing the CR distribution and known astrophysical diffuse emission and constrain these parameters by fitting the models to the *LAT gamma-ray data*.

### 3. DM maps

Numerical simulations of Milky Way size halos reveal a smooth halo which contains large number of subhalos Diemand *et al.* [2007], Springel *et al.* [2008]. The properties of the smooth halo seem to be well understood, at least on the scales resolved by simulations, while the properties of the subhalo population are more model dependent. In the inner  $\lesssim 20^\circ$  region of the Galaxy, the smooth component is expected to dominate, Diemand *et al.* [2007b], Springel *et al.* [2008b], Pieri *et al.* [2011] and we conservatively consider only the smooth component in this work.

We parametrize the smooth DM density  $\rho$  with a NFW spatial profile Navarro *et al.* [1996]

$$\rho(r) = \frac{\rho_0 R_s}{r (1 + r/R_s)^2} \quad (1)$$

and a cored (isothermal-sphere) profile Begeman *et al.* [1991]:

$$\rho(r) = \frac{\rho_0 (R_\odot^2 + R_c^2)}{(r^2 + R_c^2)}. \quad (2)$$

For the local density of DM we take the value of  $\rho_0 = 0.43 \text{ GeV cm}^{-3}$  Salucci *et al.* [2010], and the scale radius of  $R_s = 20 \text{ kpc}$  (for NFW) and  $R_c = 2.8 \text{ kpc}$  (isothermal profile). We also set the distance of the solar system from the center of the Galaxy to the value  $R_\odot = 8.5 \text{ kpc}$ . For the annihilation/decay spectra we consider three channels with distinctly different signatures: annihilation/decay into the  $b\bar{b}$  channel, into  $\mu^+\mu^-$ , and into  $\tau^+\tau^-$ . In the first case gamma rays are produced through hadronization of annihilation products and subsequent pion decay. The resulting spectra are similar for all channels in which DM produces heavy quarks and gauge bosons and this channel is therefore representative for a large set of particle physics models. The choice of leptonic channels provided by the second and third scenarios, is motivated by the dark matter interpretation Grasso *et al.* [2009] of the PAMELA positron fraction Adriani *et al.* [2008] and the *Fermi* LAT electrons plus positrons Abdo *et al.* [2009] measurements. In this case, gamma rays are

dominantly produced through radiative processes of electrons, as well as through the Final State Radiation (FSR). We produce the DM maps with a version of GALPROP slightly modified to implement custom DM profiles and injection spectra (which are calculated by using the PPPC4DMID tool described in Cirelli *et al.* [2010] and include a contribution from electro-weak bremsstrahlung).

## 4. Approach to set DM limits

We use 24 months of LAT data in the energy range between 1 and 100 GeV (but, we use energies up to 400 GeV when deriving DM limits with no assumption on the astrophysical background). We use only events classified as gamma rays in the P7CLEAN event selection and the corresponding P7CLEAN\_V6 instrument response functions (IRFs)<sup>1</sup>. Structures like Loop I and the Galactic Bubbles appear mainly at high Galactic latitudes and to limit their effects on the fitting we will consider a ROI in Galactic latitude,  $b$ , of  $5^\circ \leq |b| \leq 15^\circ$ , and Galactic longitude,  $l$ ,  $|l| \leq 80^\circ$ . We mask the region  $|b| \lesssim 5^\circ$  along the Galactic Plane, in order to reduce the uncertainty due to the modeling of the astrophysical and DM emission profiles.

### 4.1. DM limits with no assumption on the astrophysical background

To set these type of limits we first convolve a given DM model with the Fermi LAT instrument response functions (IRFs) to obtain the counts expected from DM annihilation. The expected counts are then compared with the observed counts in our ROI and the upper limit is set to the *minimum* DM normalization which gives counts in excess of the observed ones in at least one bin, i.e. we set  $3\sigma$  upper limits given by the requirement  $n_{iDM} - 3\sqrt{n_{iDM}} > n_i$ , where  $n_{iDM}$  is the expected number of counts from DM in the bin  $i$  and  $n_i$  the actual observed number of counts.

### 4.2. DM limits with modeling of astrophysical background

In this analysis we model the diffuse emission as a combination of a dark matter and a parameterized conventional astrophysical signal and we derive the limits on the DM contribution using the *profile likelihood method*.

The parameters we use to describe conventional astrophysical emission and their ranges are summarized in Table II.

<sup>1</sup><http://fermi.gsfc.nasa.gov/ssc/>

For each DM channel and mass, the model which describes the LAT data best is determined by maximizing the likelihood function defined as

$$L_k(\theta_{DM}) = L_k(\theta_{DM}, \hat{\vec{\alpha}}) = \max_{\vec{\alpha}} \prod_i P_{ik}(n_i; \vec{\alpha}, \theta_{DM}), \quad (3)$$

where  $i$  are spatial and spectral bins,  $P_{ik}$  is the Poisson distribution for observing  $n_i$  events in bin  $i$  given an expectation value that depends on the parameter set  $(\theta_{DM}, \vec{\alpha})$ .  $\theta_{DM}$  is the intensity of the DM component,  $\vec{\alpha}$  represents the set of parameters which enter the astrophysical diffuse emission model as linear pre-factors to the individual model components (cf. equation 4 below), while  $k$  denotes the set of parameters which enter in a non-linear way. We sample non-linear parameters on a grid in the  $k$  parameter space (see Table II). On each point on a grid of non-linear parameters and for each fixed value of DM normalization  $\theta_{DM}$  we find the values of linear parameters ( $\vec{\alpha}$ ) which maximize the likelihood and the value of the likelihood itself at the maximum, thus determining the curve  $L_k(\theta_{DM})$ . The outlined procedure is then repeated for each set of values of the non-linear propagation and injection parameters to obtain the full set of profile likelihood curves. We scan over the three parameters: electron injection index, the height of the diffusive halo and the gas to dust ratio which parametrizes different gas column densities (see Table II). In this way we end up with a set of  $k$  profiles of likelihood  $L_k(\theta_{DM})$ , one for each combination of the non-linear parameters. The envelope of these curves then approximates the *final* profile likelihood curve,  $L(\theta_{DM})$ , where all the parameters, linear and non-linear have been included in the profile. Limits are calculated from the profile likelihood function by finding the  $\theta_{DM,lim}$  values for which  $L(\theta_{DM,lim})/L(\theta_{DM,max})$  is  $\exp(-9/2)$  and  $\exp(-25/2)$ , for 3 and 5  $\sigma$  C.L. limits, respectively.

In each step, the maps (produced by the GALPROP code) which are used for fits, and their normalization parameters are combined as:

$$F = \sum_i \left\{ c_i^p (H_{\pi^0}^i + \sum_j X_{CO}^j H_{2\pi^0}^{ij}) + c_i^e (H_{\text{bremss}}^i + \sum_j X_{CO}^j H_{2\text{bremss}}^{ij} + IC^i) \right\} + \alpha_\chi (\chi_\gamma + \chi_{ic}) + \sum_m \alpha_{IGB,m} IGB^m. \quad (4)$$

here, the sum over  $i$  is the sum over all step-like distributions of cosmic ray source (CRSD) functions<sup>2</sup>,

the sum over  $j$  corresponds to the sum over all Galactocentric annuli (details of the procedure of a placement of the gas in Galactocentric annuli and their boundaries are given in Ackermann *et al.* [2012b]).  $H$  denotes the gamma-ray emission from atomic and ionized interstellar gas while  $H_2$  the one from molecular hydrogen<sup>3</sup> and  $IC$  the Inverse Compton emission.  $\chi_\gamma$  and  $\chi_{ic}$  are the prompt and Inverse Compton (when present) DM contribution and  $\alpha_\chi$  the overall DM normalization. Additionally an isotropic component arising from the extragalactic gamma-ray background and misclassified charged particles needs to be included to fit the *Fermi* LAT data.  $\alpha_{IGB,m}$  and  $IGB^m$  denote the Isotropic Gamma-ray Background (IGB) intensity for each of the five energy bins over which the index  $m$  runs. In all the rest of the expression the energy index  $m$  is implicit since we don't allow for the freedom of varying the GALPROP output from energy bin to energy bin. We do not include sources in the fit as we use a mask to filter point sources from the 1FGL catalog Abdo *et al.* [2010].

## 5. Results

An important point to note about our fitting procedure is that, for each DM model, the global minimum we found lies within the 3(5)  $\sigma$  regions of many different models, providing a check against a bias in our procedure. This point is illustrated in Figure 1, where the profile likelihoods for the three nonlinear parameters,  $z_h$ ,  $\gamma_{e,2}$  and d2HI, are shown. To ease reading of the figure the profiling is actually performed with further grouping DM models with different DM masses, but keeping the different DM channels, DM profiles and the annihilation/decay cases separately. The curve for the fit without DM is also shown for comparison. Each resulting curve has been further rescaled to a common minimum, since we are interested in showing that several models are within  $-2\Delta\log L \leq 25$  around the minimum for each DM fit.

DM searches. CRSDs are traditionally modeled from the direct observation of tracers of SNR and can be observationally biased. In order to circumvent this problem, we define a parametric CRSD as sum of *step functions* in Galactocentric radius  $R$ , and treat the normalization of each step as a free parameter *in the fit to gamma rays*. In addition, in order to have conservative and robust limits we set to zero the  $e, p$  CRSDs in the inner Galaxy region, within 3 kpc of the Galactic Center. In this way, potential  $e$  and  $p$  CR sources which would be required in the inner Galaxy will be potentially compensated by DM, producing conservative constraints.

<sup>3</sup>It should be noted that in our case, where we mask  $\pm 5^\circ$  along the plane, the expression actually simplifies considerably since only the local ring  $X_{CO}$  factor enters the sum, since all the other  $H_2$  rings do not extend further than 5 degrees from the plane.

<sup>2</sup>CRSD over the Galactic plane is a critical parameter for

The  $\gamma_{e,2}$  profile, for example, indicates that all models with  $\gamma_{e,2}$  from 1.9 to 2.4 are within  $-2\Delta\log L \leq 25$  around the minimum illustrating that the sampling around each of the minima for the six DM models is dense. The  $z_h$  profile indicates that basically all the considered values of  $z_h$  are close to the absolute minima. This last result is not surprising since, within our low-latitude ROI, we have little sensitivity to different  $z_h$  and basically all of them fit equally well. There is some tendency to favor higher values of  $z_h$  when DM is not included in the fit, while with DM the trend is inverted. Although the feature is not extremely significant it is potentially very interesting.

Upper limits on the velocity averaged annihilation cross section into various channels are shown in Fig. 2, for isothermal profile of the DM halo<sup>4</sup>, together with regions of parameter space which provide a good fit to PAMELA (purple) and *Fermi* LAT (blue) CR electron and positron data Cirelli *et al.* [2009].

The resulting DM limits are comparable with the limits from LAT searches for a signal from DM annihilation/decay in dwarf galaxies Ackermann *et al.* [2011]. In particular, as shown in Figure 2 for masses around 20 GeV the thermal relic value of the annihilation cross section is reached, both for the  $b\bar{b}$  and  $\tau^+\tau^-$  channels.

In addition to the parameters listed in Table II we check the importance of uncertainties in additional astrophysical parameters, but in a more simplified setup: we set a particular model as reference and then we vary each parameter one at a time, keeping the others fixed, and for each case we calculate the percentage variation in DM limits for selected DM models. We find that this produces changes in the limits of less than 10% Ackermann *et al.* [2012]. Overall, rather than being due to residual astrophysical model uncertainties, the remaining major uncertainties in the DM constraints from the Halo region come from the modeling of the DM signal itself. The main uncertainty is in the normalization of the DM profile, which is fixed through the local value of the DM density. We use the recent determination  $\rho_0 = 0.43 \text{ GeV cm}^{-3}$  from Salucci *et al.* [2010], which has, however, a large uncertainty, with values in the range 0.2-0.7  $\text{GeV cm}^{-3}$  still viable. A large uncertainty in  $\rho_0$  is particularly important for annihilation constraints since they scale like  $\rho_0^2$ , while for constraints on decaying DM the scaling is only linear. A less important role is played by the uncertainties in the DM profile, since in our region of interest different profiles predict similar DM densities.

## References

- M. Ackermann *et al.* [The Fermi-LAT collaboration], *Astrophys. J.* **761**, 91, 2012.
- M. Ackermann *et al.* [The Fermi-LAT collaboration], *Astrophys. J.*, **750**, 3 (2012),
- A. W. Strong, I. V. Moskalenko and O. Reimer, *Astrophys. J.* **537**, 763 (2000), url: <http://galprop.stanford.edu/webrun.php>.
- J. -M. Casandjian, I. Grenier [The Fermi-LAT collaboration], [arXiv:0912.3478 [astro-ph.HE]]. (2009)
- M. Su, T. R. Slatyer, D. P. Finkbeiner, *Astrophys. J.* **724**, 1044-1082 (2010).
- J. Diemand, M. Kuhlen and P. Madau, *Astrophys. J.* **667** (2007) 859
- V. Springel *et al.*, *Mon. Not. Roy. Astron. Soc.* **391**, 1685 (2008)
- J. Diemand, M. Kuhlen and P. Madau, *Astrophys. J.* **657** (2007) 262
- V. Springel, S. D. M. White, C. S. Frenk, J. F. Navarro, A. Jenkins, M. Vogelsberger, J. Wang and A. Ludlow *et al.*, arXiv:0809.0894 [astro-ph] (2008).
- L. Pieri, J. Lavalle, G. Bertone and E. Branchini, *Phys. Rev. D* **83**, 023518 (2011)
- J. F. Navarro, C. S. Frenk and S. D. M. White, *Astrophys. J.* **462**, 563 (1996).
- K. G. Begeman, A. H. Broeils and R. H. Sanders, *Mon. Not. Roy. Astron. Soc.* **249**, 523 (1991).
- P. Salucci, F. Nesti, G. Gentile, C. F. Martins, *Astron. Astrophys.* **523**, A83 (2010).
- D. Grasso *et al.* [FERMI-LAT Collaboration], *Astropart. Phys.* **32**, 140 (2009). P. Meade, M. Papucci, A. Strumia and T. Volansky, *Nucl. Phys. B* **831**, 178 (2010). L. Bergstrom, J. Edsjo and G. Zaharijas, *Phys. Rev. Lett.* **103**, 031103 (2009).
- O. Adriani *et al.* [PAMELA Collaboration], *Nature* **458**, 607 (2009).
- A. A. Abdo *et al.* [The Fermi LAT Collaboration], *Phys. Rev. Lett.* **102**, 181101 (2009).
- M. Cirelli *et al.*, *JCAP* **1103** (2011) 051.
- A. A. Abdo *et al.* [The Fermi-LAT collaboration], *Astrophys. J. Suppl.* **188** (2010) 405-436.
- M. Cirelli, P. Panci, P. D. Serpico, *Nucl. Phys.* **B840** (2010) 284-303.
- M. Ackermann *et al.* [Fermi-LAT Collaboration], *Phys. Rev. Lett.* **107**, 241302 (2011).

---

<sup>4</sup>Limits obtained using the NFW profile are only slightly better.

Table I Paramateres

Non linear Parameters	Symbol	Grid values
index of the injection CRE spectrum	$\gamma_{e,2}$	1.800, 1.925, 2.050, 2.175, 2.300, 2.425, 2.550, 2.675
half height of the diffusive halo	$z_h$	2, 4, 6, 8, 10, 15 kpc
dust to HI ratio	d2HI	$(0.0120, 0.0130, 0.0140, 0.0150, 0.0160, 0.0170) \times 10^{-20} \text{ mag cm}^2$
Linear Parameters	Symbol	Range of variation
eCRSD and pCRSD coefficients	$c_i^e, c_i^p$	$0, +\infty$
local H <sub>2</sub> to CO factor	$X_{CO}^{loc}$	$0\text{-}30 \times 10^{20} \text{ cm}^{-2} (\text{K km s}^{-1})^{-1}$
IGB normalization in various energy bins	$\alpha_{IGB,m}$	free
DM normalization	$\alpha_\chi$	free

Table II Summary table of the parameters varied in the fit. The top part of the table show the non linear parameters and the grid values at which the likelihood is computed. The bottom part show the linear parameters and the range of variation allowed in the fit. The coefficients of the CRSDs are forced to be positive, apart  $c_1^{e,p}$  and  $c_2^{e,p}$  which are set to zero. The local  $X_{CO}$  ratio is restricted to vary in the range  $0\text{-}30 \times 10^{20} \text{ cm}^{-2} (\text{K km s}^{-1})^{-1}$ , while  $\alpha_{IGB,m}$  and  $\alpha_\chi$  are left free to assume both positive and negative values. See the text for more details.

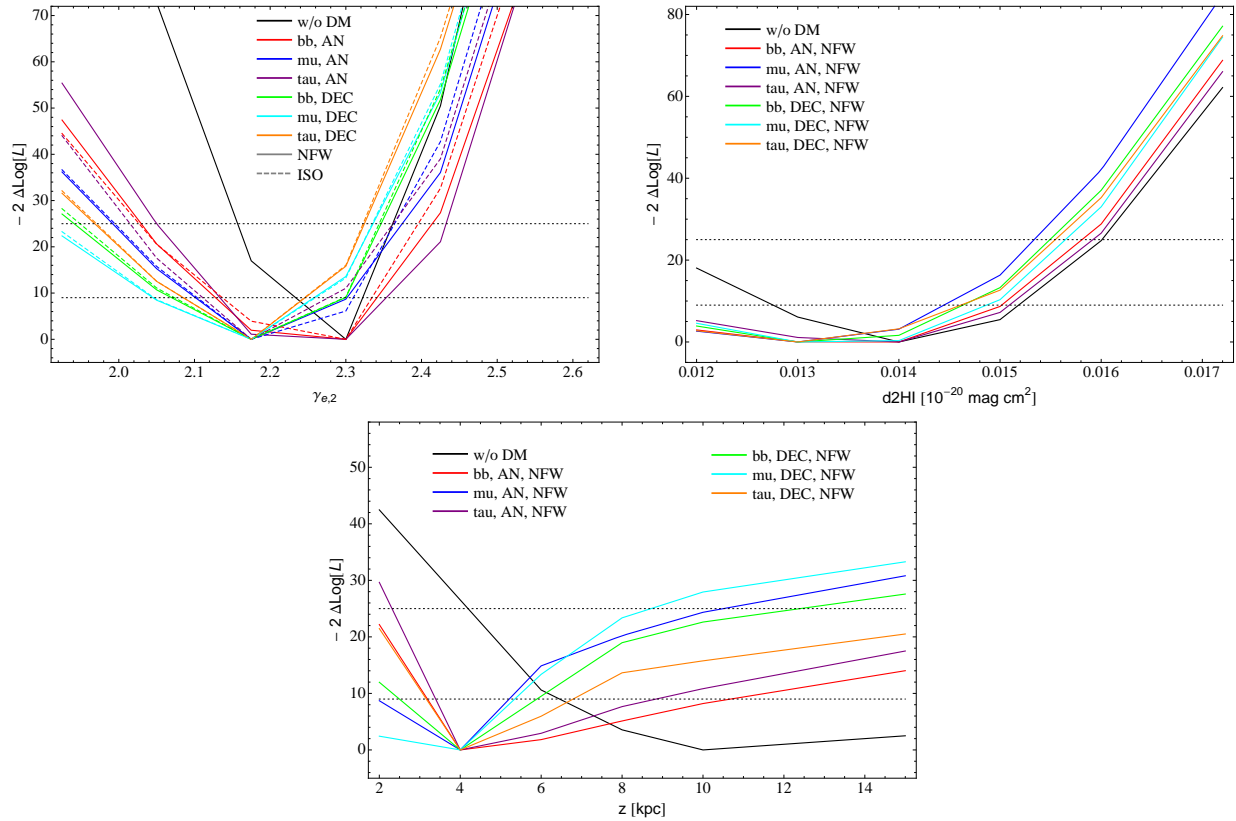


Figure 1: Profile likelihood curves for  $z_h$ ,  $\gamma_{e,2}$  and d2HI. The various curves refer to the case of no DM or different DM models (see the legend in the figure, where we mark a dominant decay (DEC) or annihilation (AN) channel and the assumed DM profile). All minima are normalized to the same level. Horizontal dotted lines indicate a difference in  $-2\Delta\log L$  from the minimum of 9 ( $3\sigma$ ) and 25 ( $5\sigma$ ).

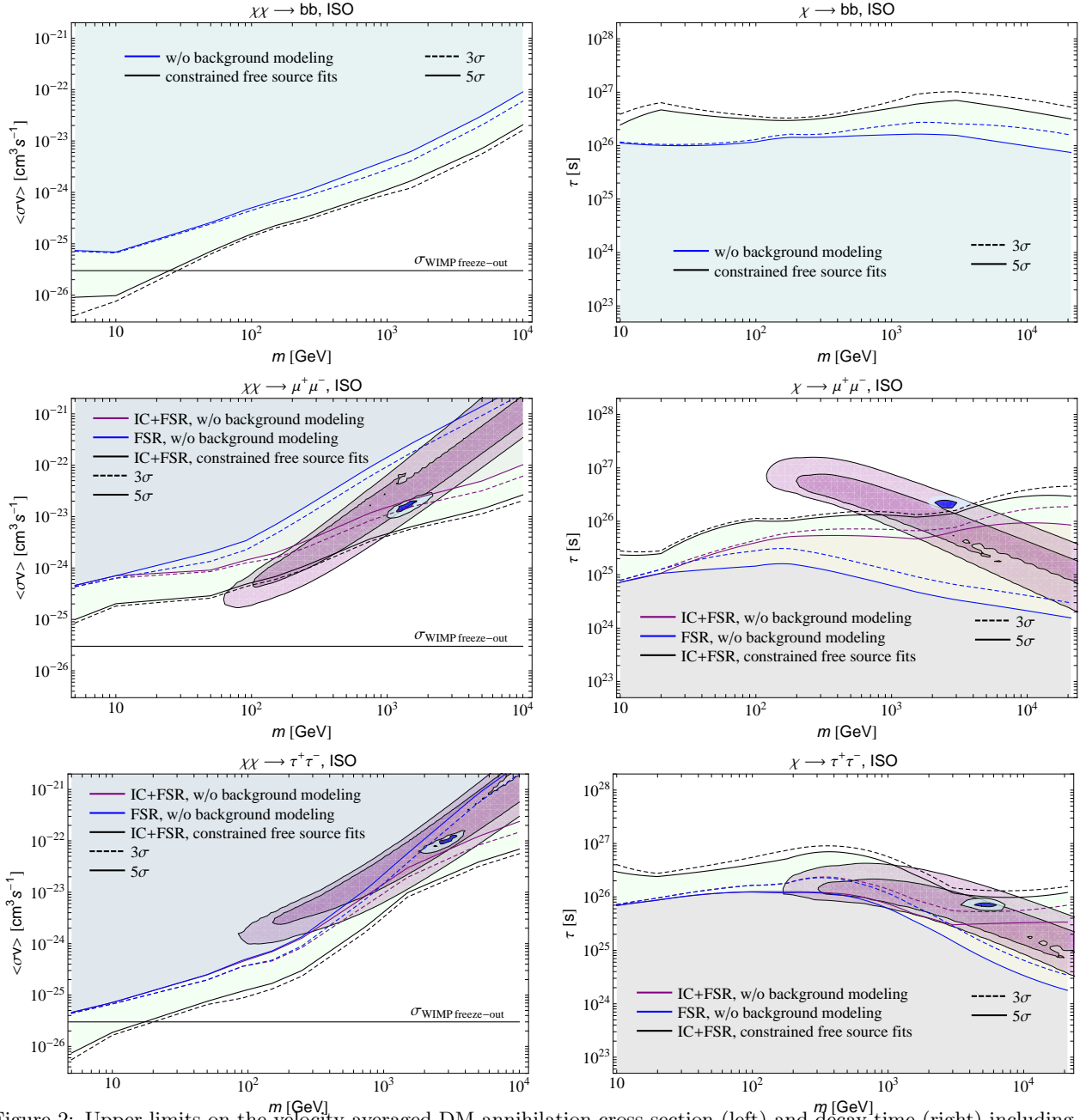


Figure 2: Upper limits on the velocity averaged DM annihilation cross-section (left) and decay time (right) including a model of the astrophysical background compared with the limits obtained with no modeling of the background. Limits are shown for  $b\bar{b}$  (upper),  $\mu^+\mu^-$  (middle) and  $\tau^+\tau^-$  (lower panel) channels, for a DM distribution given by the isothermal distribution. The horizontal line marks the thermal decoupling cross section expected for a generic WIMP candidate. The regions of parameter space which provide a good fit to PAMELA (purple) and *Fermi* LAT (blue) CR electron and positron data are also shown.